EUROPEAN JOURNAL OF COMPUTATIONAL MECHANICS
2018, VOL. 27, NOS. 5–6, 383–400
https://doi.org/10.1080/17797179.2018.1469834

Taylor & Francis
Taylor & Francis Group



# Inverse Green element simulations of instantaneous pollutant injections into a 2-D aquifer

Akpofure Taigbenu

School of Civil & Environmental Engineering, University of the Witwatersrand, Johannesburg, South Africa

**ABSTRACT**

When pollution spills occur, they impact on the quality of water in underlying aquifers. Such spills can be modelled as instantaneous pollution sources, and estimating their strengths from the concentration plumes they produce is an inverse problem which is addressed in this paper by the Green element method (GEM). Estimating the strengths of such spills, making use of the concentration data at various locations and times, is an inverse problem whose solution is often associated with non-uniqueness, non-existence and instability. Here the GEM is used to predict the strengths of pollution spills from measured concentration data at internal observation points. The performance of the methodology is illustrated using two numerical examples in which the contaminant plumes are from multiple point and distributed pollution sources. Single and multiple episodes of pollution injections are accommodated in both examples. It is observed that GEM is more accurate in predicting the strengths of distributed instantaneous pollution sources than point sources because of the discontinuities of the latter in both the spatial and temporal dimensions.

**ARTICLE HISTORY**
Received 30 November 2017
Accepted 12 April 2018

**KEYWORDS**
The Green element method; inverse simulations; point & distributed instantaneous pollution injections; Tikhonov regularisation

## 1. Introduction

Injections of pollutants into groundwater systems do occur on a regular basis. These injections can be intentional or accidental. When they occur over a very small interval of time, they can be considered to be instantaneous, but when they occur over a prolonged period of time, they are then referred to as being continuous. The former is the subject of this paper. The impacts of such instantaneous pollution injections on groundwater systems persist over spatial and temporal scales that are considerably much larger than those of the pollutant source as the pollutants undergo various chemical and hydrodynamic processes. It is common to observe these impacts in downstream wells and surface water bodies after

**CONTACT** Akpofure Taigbenu akpofure.taigbenu@wits.ac.za

months or years of the occurrence of the spills. Forensic or inverse groundwater modelling uses pollution concentration information at different observation points in time to predict the strength of the pollution spill. The numerical challenges presented by such inverse modelling exercises are that many solutions could exist which satisfy the recreated contamination scenario, and the numerical solution could be unstable.

There is a wide variety of inverse groundwater contaminant transport problems that present themselves in practice, and their solutions have generally been addressed by stand-alone simulation techniques or combined simulation and optimization techniques or some variants of these (Atmadja & Bagtzoglou, 2001; Michalak & Kitanidis, 2004; Sun, Painter, & Wittmeyer, 2006a, 2006b). Most of the inverse solution techniques have addressed groundwater contaminant transport with continuous pollution injections (Atmadja, & Bagtzoglou, 2001; Datta, Chakrabarty, & Dhar, 2011; Jha & Datta, 2013).

There are fewer attempts at inverse numerical simulations to estimate the pollution source strength from instantaneous injection of contaminants into aquifers (Cokca, Bilge, & Unutmaz, 2009; Neupauer & Lin, 2006). Such problems have singularities in the temporal dimension because the pollutant is released in an infinitesimal time interval and, for problems with point pollution injections, there is the additional challenge of spatial discontinuity in the vicinity of the source. In this paper, the Green element formulation, presented in Taigbenu (2012) that had been been applied to inverse solution of groundwater contaminant transport with continuous pollution injection (Onyari & Taigbenu, 2017), is used in conjunction with Tikhonov regularisation to predict the strengths of point and distributed sources instantaneously introduced into an aquifer. The Green element method (GEM) is founded on the singular integral theory of the boundary element method (BEM) and it implements the theory in an element-by-element manner like in the finite element method (FEM). This approach achieves a resultant global coefficient matrix that is banded, and has the added advantages of ease of solution of nonlinear problems in heterogeneous domains and those with point and distributed singularities. The inverse simulations use the concentration information at observation points to enhance the numerical solutions. Two numerical examples of transient contaminant transport in 2-D aquifers are used to demonstrate the capability of the methodology. The first example relates to instantaneous injections of pollutants at point sources, while the second relates to instantaneous injections at distributed sources. In both examples, the performances of the inverse Green element formulation are evaluated when there is a single episode of injections and when there are multiple episodes of injections. The formulation provides more stable and reliable estimates of the pollution source strengths for distrbuted sources than point sources.

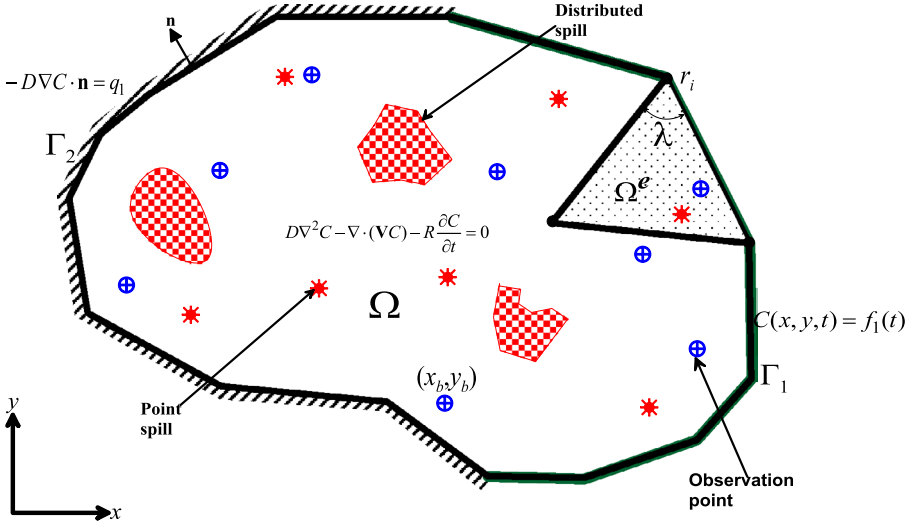


Figure 1. Schematic of the problem statement.

## 2. Contaminant transport equation

The transient contaminant transport equation in a 2-D aquifer is addressed in this paper. The equation describes the spread of the pollutant due to hydrodynamic dispersion, its advection as it is transported by the ambient flow field and as well the temporal variation of its concentration. The governing equation for an incompressible aquifer is (Bear, 1979):

$$\nabla\cdot(D\nabla C)-\nabla C\cdot\mathbf{V}-R\frac{\partial C}{\partial t}=0 \tag{1}$$

where $\nabla=\partial/\partial x\mathbf{e}_x+\partial/\partial y\mathbf{e}_y$ is the 2-D gradient operator with unit vectors $\mathbf{e}_x$ and $\mathbf{e}_y$ in the spatial directions $x$ and $y$, $C=C(x,y,t)$ is the concentration in time and space in the domain $\Omega$, $\mathbf{V}=u\mathbf{e}_x+v\mathbf{e}_y$ is the flow velocity vector, $D$ is the hydrodynamic dispersion coefficient and $R$ is the retardation factor which, in the test cases addressed in this paper, assumes a value of unity. The inverse problem that is addressed solves Equation (1) subject to the Dirichlet and Neumann boundary conditions:

$$C(x,y,t)=f_1 \text{ on } \Gamma_1 \tag{2}$$

$$-D\nabla C\cdot\mathbf{n}=q_1 \text{ on } \Gamma_2 \tag{3}$$

in which $\mathbf{n}$ is the unit outward pointing normal vector, and $\Omega$ is the domain with boundary $\Gamma=\Gamma_1\cup\Gamma_2$ (Figure 1). On the piece-wise smooth boundary in Figure 1, $n$ does not exist everywhere but only along the smooth segment of the boundary. The initial condition reflects either instantaneous point pollution sources that are described by the relationship

$$C(x,y,0) \equiv C(r,0) = \sum_{i=1}^{P} S_i \delta(r - r_i) \tag{4a}$$

or instantaneous distributed pollution sources that are described as

$$C(x,y,0) \equiv C(r,0) = \sum_{i=1}^{P} S_i(r) \tag{4b}$$

where $S_i$ is the pollution source strength of the injection into the aquifer and $P$ is the number of sources . It is expected that the inverse simulation predicts the source strength $S_i$ and it is assumed that the spatial characteristics of the source are known. There are available measured data on the concentration at $B$ number of observation points, $(x_b,y_b)$ which, in practice, could be plagued with human errors and/or measurement deficiencies. These errors are expressed as

$$\tilde{C}_b \equiv \tilde{C}(x_b, y_b, t) = C(x_b, y_b, t)\left[1 + \phi \times RAN(b)\right] \tag{5}$$

where $\varphi$ is the noise level, and $RAN$ represents random numbers and $\tilde{C}_b$ is the perturbed value of the observed concentration $C_{b=}C(x_b,y_b)$.

## 3. Inverse Green element formulation

Equation (1) is solved in a homogeneous aquifer so that it becomes:

$$D\nabla^2 C - \nabla C \cdot \mathbf{V} - R\frac{\partial C}{\partial t} = 0 \tag{6}$$

The complementary differential equation to (6) in an infinite space in two dimensions is

$$\nabla^2 G = \delta\left(r - r_i\right) \tag{7}$$

where $\delta$ is the Dirac delta function, $r = (x,y)$ is the field point and $r_i = (x_i,y_i)$ is the collocation point. The solution to Equation (7) is well known; it is $G_i = \ln(r - r_i)$ which is has a singularity at $r_i$. With the application of Green's second identity to Equations (6) and (7), the following integral equation is obtained.

$$D\left(-\lambda C_i + \int_\Gamma C\frac{\partial G}{\partial n} ds\right) + \int_\Gamma G\, q\, ds + \iint_\Omega G\left[\left(R\frac{\partial C}{\partial t} + \mathbf{V} \cdot \nabla C\right)\right] dA = 0 \tag{8}$$

where $C_i = C(r_i)$ and $\lambda$ is the nodal angle at $r_i$, and $q = -D\partial C/\partial n$ is the normal contaminant flux. Equation (8) is the classical integral equation that emerges in the singular integral theory of the BEM (Brebbia, 1978). It is however implemented in

the finite element sense by discretizing the computational domain into polygonal elements over which the quantities $C$, $\mathbf{V}$ and $q$ are approximated by basis functions of the Lagrange family ($C \approx N_j C_j$). In this work, rectangular elements and linear basis functions are used. The discrete element equation for each element $\Omega^e$ with boundary $\Gamma^e$ is

$$V_{ij}C_j + L_{ij}q_j + W_{ij}R\frac{dC_j}{dt} + U_{ikj}u_k C_j + Y_{ikj}v_k C_j = 0 \tag{9}$$

where

$$\begin{aligned} V_{ij} &= D\left(\int_{\Gamma^e} N_j \nabla G_i - \delta_{ij}\lambda\right), \quad L_{ij} = \int_{\Gamma^e} N_j G_i ds, \quad W_{ij} = \iint_{\Omega^e} N_j G_i dA, \\ U_{ikj} &= \iint_{\Omega^e} G_i N_k \frac{\partial N_j}{\partial x} dA, \quad Y_{ikj} = \iint_{\Omega^e} G_i N_k \frac{\partial N_j}{\partial y} dA \end{aligned} \tag{10}$$

The nodal angle $\lambda$ at $r_i$ is indicated in Figure 1 for the element $\Omega^e$ with boundary $\Gamma^e$. The discrete element equation (9) is aggregated for all elements used in discretizing the computational domain, and the temporal term is approximated by a finite difference approximation in time, that is, $dC/dt \approx [C^{(2)}-C^{(1)}]/\Delta t$ at the time $t = t_{1+}\theta\Delta t$, where $0 \le \theta \le 1$ is the weighting factor and $\Delta t$ is the time step between the current time $t_2$ and the previous time $t_1$. With this approximation, Equation (9) becomes

$$\theta E_{ij}C_j^{(2)} + R\frac{W_{ij}}{\Delta t}C_j^{(2)} + \omega E_{ij}C_j^{(1)} - R\frac{W_{ij}}{\Delta t}C_j^{(1)} + \theta L_{ij}q_j^{(2)} + \omega L_{ij}q_j^{(1)} = 0 \tag{11}$$

where $E_{ij} = V_{ij} + U_{ikj}u_k + Y_{ikj}v_k$, $\omega = 1 - \theta$, and the superscripts represent the times at which the quantities are evaluated. The instantaneous releases of pollutants into the aquifer, described by Equations (4a) and (4b), have to be accounted for in Equation (9). The point sources that are instantaneously injected at $t = t_1$ are accounted for by implementing the term $R\frac{W_{ij}}{\Delta t}C_j^{(1)}$ in Equation (9), and this is achieved in the following manner.

$$\frac{R}{\Delta t}\iint_{\Omega} GC(r,0)dA = \frac{R}{\Delta t}\iint_{\Omega}\sum_{j=1}^{P} S_j\delta(r-r_j)\ln(r-r_j)dA = \frac{R}{\Delta t}\sum_{j=1}^{P} S_j \ln(r_i - r_j) \tag{12}$$

It is observed in Equation (12) that we have taken advantage of the property of the Dirac delta function in the evaluation of the integral, and the contribution of an instantaneous point injection is the Logarithm of the absolute value of the distance between the collocation point and the pollution source location. For

distributed sources instantaneously injected into the aquifer at $t = t_1$, then $R\frac{W_{ij}}{\Delta t}C_j^{(1)}$ is evaluated by the relationship

$$\frac{R}{\Delta t}\iint_{\Omega} GC(r,0)dA = \frac{R}{\Delta t}\iint_{\Omega}\sum_{j=1}^{P} S_j(r)\ln(r-r_j)dA = \frac{R}{\Delta t}\sum_{j=1}^{P} W_{ij}S_j \tag{13}$$

It is observed in Equation (13) that the elemental matrix $W_{ij}$, whose expression is presented in Equation (10), is used in accounting for the source strength. Equation (11) is now simplified to

$$\theta E_{ij}C_j^{(2)} + R\frac{W_{ij}}{\Delta t}C_j^{(2)} + H_{ij}S_j + \theta L_{ij}q_j^{(2)} = -\omega E_{ij}C_j^{(1)} - \omega L_{ij}q_j^{(1)} \tag{14}$$

where $H_{ij}$ denotes the matrix that captures the contribution of the instantaneous pollution sources. The global matrix equation of (14) is achieved by retaining the concentration, $C$, and contaminant flux, $q$, at the external nodes, and expressing the latter in terms of the former at the internal nodes so that only $C$ is calculated at the internal nodes. The procedure to achieving this is described in Taigbenu (2012). In a condensed form, Equation (14) is expressed as

$$\mathbf{Pz} = \mathbf{f} \tag{15}$$

where

$$\mathbf{P} = \begin{bmatrix} \theta E_{ij} + R\frac{W_{ij}}{\Delta t} \\ \theta L_{ij} \\ H_{ij} \end{bmatrix} \text{and } \mathbf{z} = \begin{Bmatrix} C_j^{(2)} \\ q_j^{(2)} \\ S_j \end{Bmatrix} \tag{16}$$

where $\mathbf{P}$ is an $M \times N$ matrix, with $M$ being the number of nodes or collocation points in the computational domain which is the same as the number of discrete equations generated, and $N$ represents the number of unknowns in the vector $\mathbf{z}$ which are $C_j$ and/or $q_j$ at external nodes, $C_j$ at internal nodes where measurement data are not available, and the pollution sources, $S_j$. The vector $\mathbf{f}$ represents the known quantities which consist of the terms on the right hand side of Equation (14) and as well as the contributions from the available concentration measurements. Equation (15) is generally an over-determined, ill-conditioned system of equations which is solved by the least squares method and regularised by the Tikhonov regularisation technique. We have achieved improved stability of the regularisation technique by decomposing the matrix $\mathbf{P}$ by the singular value decomposition (SVD) technique. This gives

$$\mathbf{P} = \mathbf{UDV}^{tr} = \sum_{i=1}^{N} \sigma_i u_i v_i^{tr} \tag{17}$$

where $\mathbf{U}$ and $\mathbf{V}$ are $M \times M$ and $N \times N$ orthogonal matrices, $u_i$ and $v_i$ are respectively the column vectors of $\mathbf{U}$ and $\mathbf{V}$, and $\boldsymbol{D}$ is an $M \times N$ diagonal matrix with $N$ non-negative diagonal elements of singular values $\sigma_i$ ($\mathbf{D} = diag\ (\sigma_1, \sigma_2, \ldots \sigma_N)$) which satisfy the condition: $\sigma_1 > \sigma_2 > \cdots > \sigma_N > 0$. The least squares solution of Equation (15) with Tikhonov regularisation minimises the Euclidean norm $\|\mathbf{Pz} - \mathbf{f}\|^2 + \alpha^2 \|\mathbf{z}\|^2$ in computing the solution of $\mathbf{z}$ which is given as;

$$\mathbf{z}(\alpha) = \sum_{i=1}^{N} \frac{\sigma_i}{\alpha^2 + \sigma_i^2} u_i^{tr} \mathbf{f} v_i \tag{18}$$

where $\alpha$ is the regularisation parameter, and the factor $\sigma_i/(\alpha^2 + \sigma_i^2)$ plays the role of dampening the instability caused by the small singular values which tend to have considerable influence on the quality of the numerical solutions. The choice of the value of $\alpha$ is facilitated by the L-curve technique which is a graphical tool that identifies the suitable compromise of the norms of $\|\mathbf{Pz} - \mathbf{f}\|^2$ and $\|\mathbf{z}\|^2$ (Hansen, 1994). In this work, the optimum values of the regularisation parameter are automatically obtained from the code of the L-curve technique that has been incorporated into the current GEM formulation.

## 4. Numerical examples and discussion of results

Two numerical examples are employed to demonstrate the capabilities of the inverse Green element formulation in predicting the strengths of pollution sources that are instantaneously injected into an aquifer. In the two examples, single and multiple injection episodes are examined. The first example arises from instantaneous injection of pollutants from four point sources, and it has an exact solution which is used as a benchmark for the numerical solutions. The second example addresses distributed instantaneous pollution sources in an aquifer. The accuracy assessments of the numerical solutions in relation to benchmark solutions are evaluated by the mean error between the calculated nodal concentrations and their benchmark values using the equation

$$\varepsilon = \frac{1}{M} \sqrt{\frac{\sum_{i=1}^{M} \left( C_i^{(b)} - C_i^{(n)} \right)^2}{\sum_{i=1}^{M} C_i^{(b)2}}} \times 100 \tag{19}$$

where the superscripts $(b)$ and $(n)$ refer to the benchmark and numerical solutions.

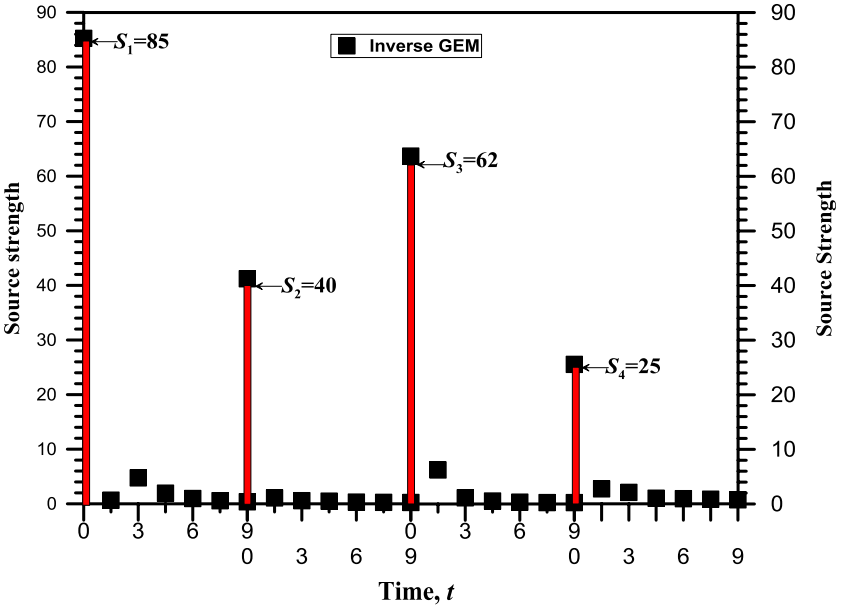


Figure 2. Exact and inverse GEM solutions for instantaneous point source strengths of Example 1 with injection at $t = 0$.

### 4.1. Example 1 of point pollution sources

#### 4.1.1. Single injection episode

This example relates to the instantaneous release of contaminants from four point sources ($p = 4$) in a 2-D homogenous aquifer that is infinitely extensive. The flow in the aquifer is in the $x$-direction with a uniform velocity $u$. The exact solution for the spatial and temporal distribution of the concentration plume is given by Bear (1979)

$$C(x,y,t) = \frac{R}{4\pi Dt}\sum_{j=1}^{4} S_j \exp\left(-\frac{R}{4Dt}\left[\left(x - x_j - \frac{ut}{R}\right)^2 - \left(y - y_j\right)^2\right]\right) \quad (20)$$

The flow and aquifer property values used in the simulations are: $u = .5$, $D = 1.0$ and $R = 1.0$. The inverse Green element simulations are carried out on a rectangular domain [50 × 20] with the values of the contaminant flux, obtained from Equation (20), prescribed on the top and bottom boundaries, while the left and right boundaries are Dirichlet boundaries with concentration values obtained from Equation (20). The analytical solution is generated with pollution source strengths $S_1 = 85.0$ at $(x_1 = 4.5, y_1 = 6.0)$, $S_2 = 40.0$ at $(x_2 = 13.0, y_2 = 16.0)$, $S_3 = 62.0$ at $(x_3 = 21.0, y_3 = 8.0)$ and $S_4 = 25.0$ at $(x_4 = 28.0, y_4 = 11.0)$. The domain is discretised into 160 uniform rectangular elements each $[\Delta x = 2.5 \times \Delta y = 2.5]$, a uniform time step $\Delta t = 1.5$, and a weighting factor, $\theta = .75$ are adopted in the simulations. We achieved better prediction of the source strength with GEM when the source

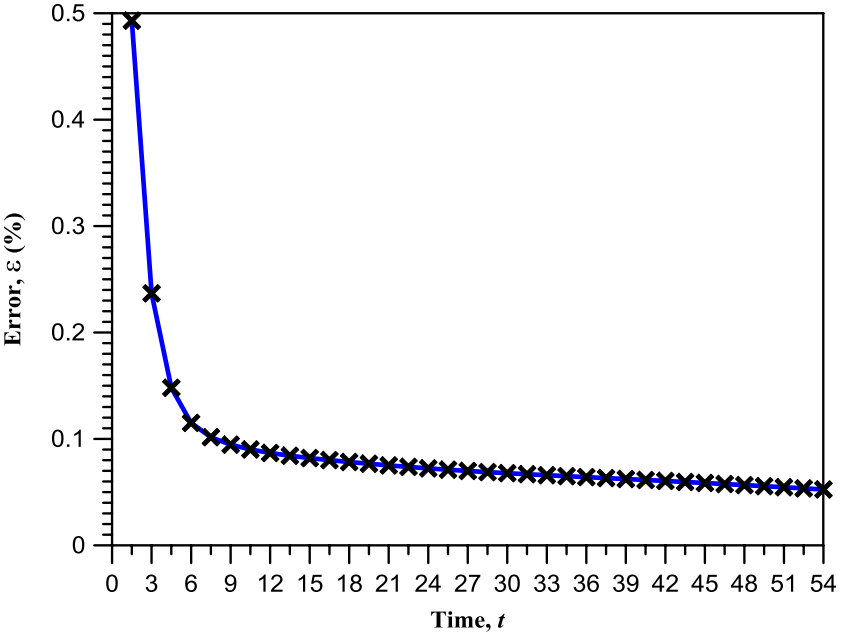


**Figure 3.** Variation of error of the GEM predicted contaminant plume with time for Example 1 with a single episode of pollutant injection at $t = 0$.

location is centred within the element. A minimum of 4 observation points is required to solve for the strengths of the pollution sources, and these are placed close to the locations of the pollution sources and on their downstream end. The observation points are at (5.0,5.0), (15.0,15.0), (22.5,7.5) and (30.0,10.0).

The inverse GEM predictions of the strengths of the four point sources in comparison with their exact values are presented in Figure 2. There is good prediction of the pollution source strength by GEM at $t = 0$, but residual sources remain for about five time steps. Whereas the source strengths should theoretically become zero for $t > 0$, the residual source strengths are due to the spatial and temporal discontinuities that arise from point sources which are only active at an infinitesimal time interval. The optimal values of the regularisation parameter range used in the simulations range between $5.48 \times 10^{-6}$ and $4.99 \times 10^{-5}$ with an average value of $2.05 \times 10^{-5}$.

The variation of the mean error $\varepsilon$ at every simulation time step is presented in Figure 3. It is observed that the errors are quite small and they decrease exponentially with time, which suggests that the inverse GEM prediction of the contaminant plume is excellent.

The contaminant plumes of the exact and the inverse GEM solutions are presented in Figure 4(a) and (b) at $t = 6$ and $t = 36$, respectively, and there is good agreement between the solutions.

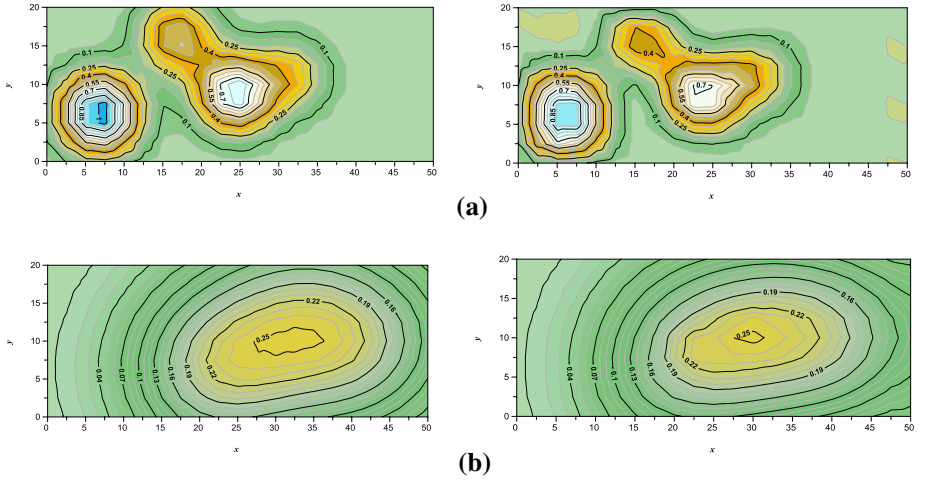


**Figure 4.** Contaminant plume of Example 1 with a single episode of pollutant injection at $t = 0$: (a) $t = 6$ and (b) $t = 36$; Exact on the left and GEM on the right.

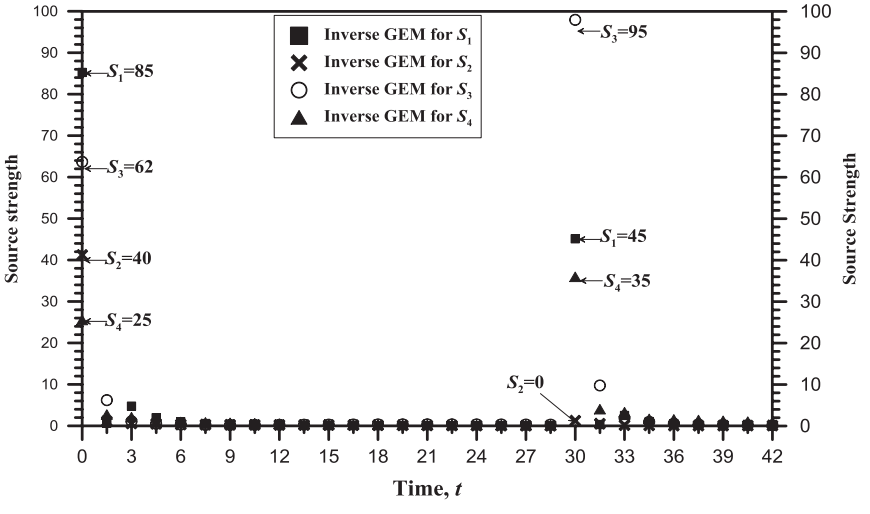


**Figure 5.** Exact and inverse GEM solutions for instantaneous point source strengths of Example 1 with injections at $t = 0$ and $t = 30$.

### *4.1.2. Multiple injection episodes*

This case is similar to the previous one except that at $t = 30$ there is another episode of pollution injection into the aquifer at three points with strengths $S_1 = 45.0$ at $(x_1 = 4.5, y_1 = 6.0)$, $S_2 = 0.0$ at $(x_2 = 13.0, y_2 = 16.0)$, $S_3 = 95.0$ at $(x_3 = 21.0, y_3 = 8.0)$ and $S_4 = 35.0$ at $(x_4 = 28.0, y_4 = 11.0)$. It is only at source point 2 that there is no re-injection of pollutants. The analytical solution is

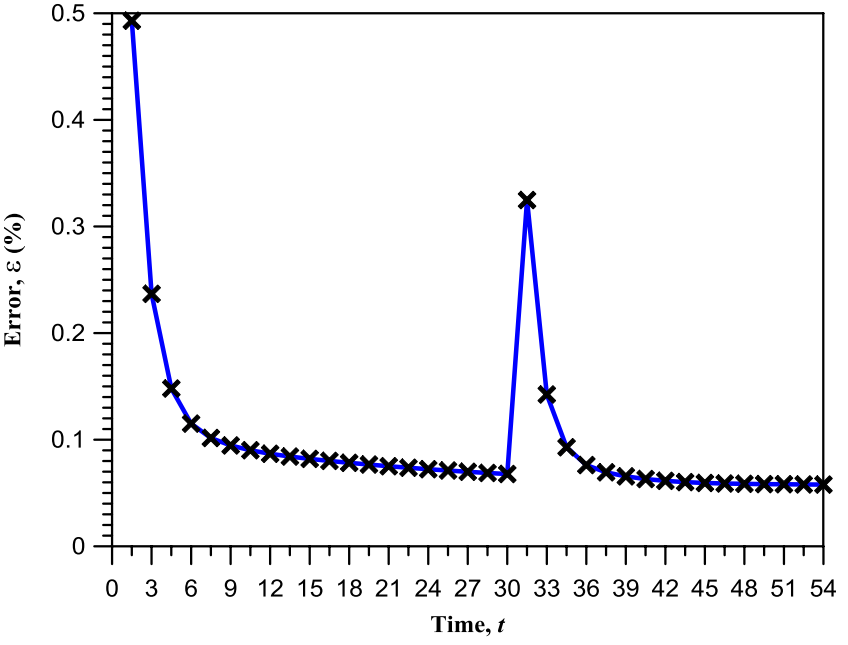


**Figure 6.** Error variation of the GEM predicted contaminant plume with time for Example 1 with multiple episodes of pollutant injection at $t = 0$ and $t = 30$.

$$C(x,y,t) = \frac{R}{4\pi tD}\left\{\begin{array}{l}\displaystyle\sum_{j=1}^{4} S_j \exp\left(-\frac{R}{4tD}\left[\left(x - x_j - \frac{ut}{R}\right)^2 - \left(y - y_j\right)^2\right]\right) + \\ \displaystyle\sum_{j=1}^{4} S_j \exp\left(-\frac{R}{4tD}\left[\left(x - x_j - \frac{u(t-30)}{R}\right)^2 - \left(y - y_j\right)^2\right]\right)\end{array}\right\} \tag{21}$$

Using the same simulation parameters as in the previous case, the pollution source strengths that are predicted by GEM are presented in Figure 5 alongside the exact solutions. The GEM formulation correctly captures the injections of pollutants at both times and, as in the previous case, there are residual sources which linger for a few time steps after the times of injections.

The variation of the error of the inverse GEM solutions for the contaminant plume in relation to the exact solutions, calculated by Equation (19), is presented in Figure 6. The error decreases exponentially till there is an episode of pollutant injection at the sources when a sharp increase in the error is observed and then decreases with time thereafter.

The contaminant plumes of the exact and the inverse GEM solutions are presented in Figure 7(a) and (b) at $t = 36$, respectively, and there is good agreement in the solutions. The contrasts in the contaminant plumes at $t = 36$, presented in Figures 4(b) and 7, underscore the impacts of a subsequent episode of pollution

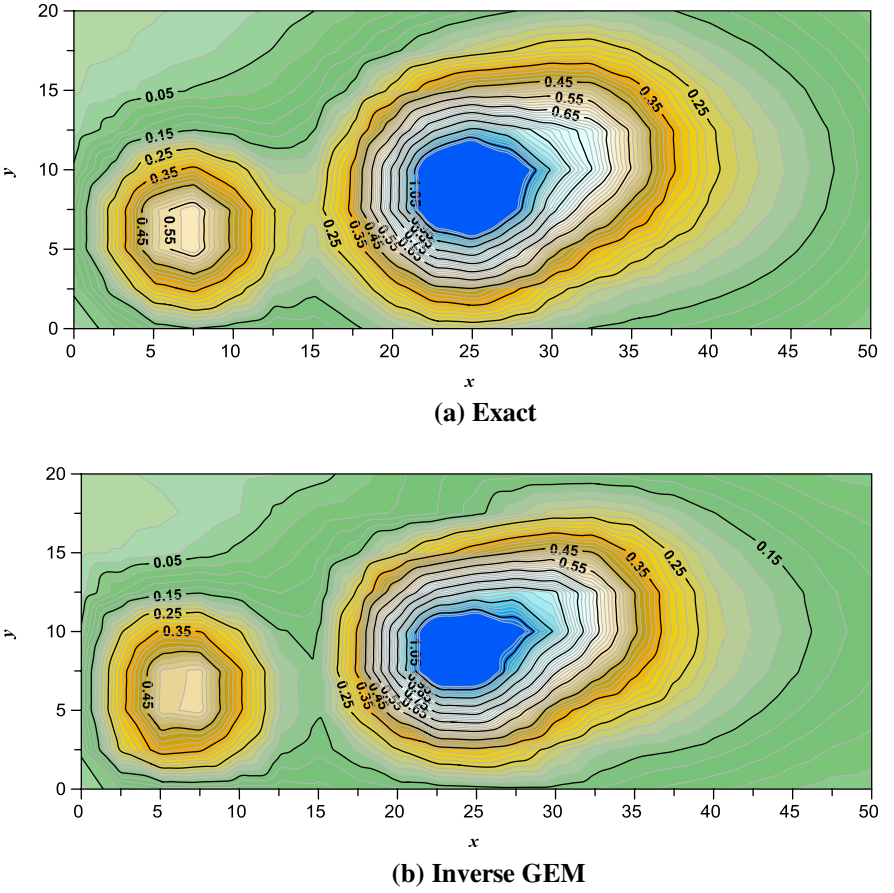


Figure 7. Contaminant plume at $t = 36$ of Example 1 with double episodes of pollutant injection at $t = 0$ and $t = 30$.

injections on the aquifer. The values of the regularisation parameter that are used in the simulations range between $4.21 \times 10^{-6}$ and $7.01 \times 10^{-5}$ with an average value of $2.12 \times 10^{-5}$.

## 4.2. Example 2 of distributed pollution sources

### 4.2.1. Single injection episode

This example is a case of instantaneous release of contaminants from three areas in the 2-D homogenous aquifer shown in Figure 8. The flow in the aquifer is in the $x$-direction with a uniform velocity $u$. The values of the aquifer and flow parameters used in numerical simulations are: $D = 400$ m$^2$/day, $R = 1.0$ and $u = 6$ m/day. The computational domain is rectangular [1200 m × 800 m], and it is assumed initially before the distributed spills that the concentration everywhere in the aquifer is .1 mg/$l$. The top and bottom boundaries are considered as no-flux boundaries, while the left boundary has a concentration of .1 mg/$l$ and the right boundary

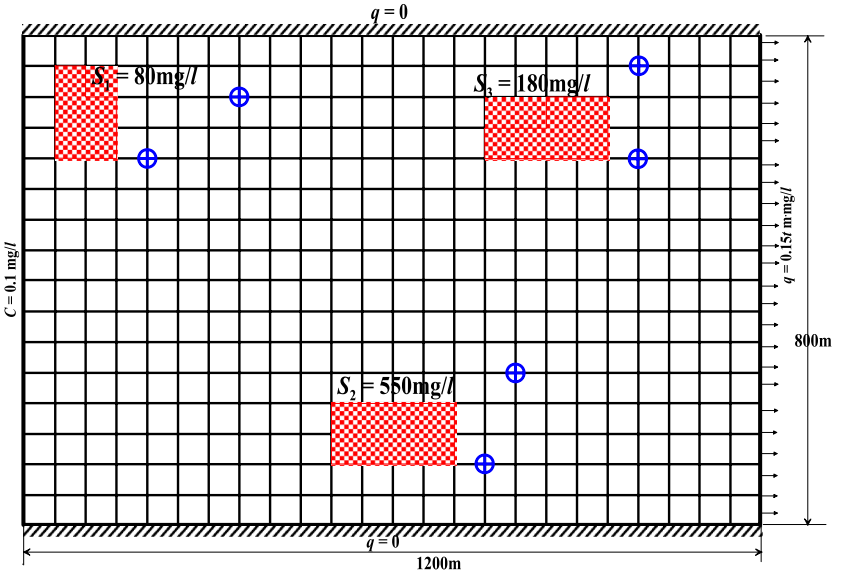


**Figure 8.** Computational domain of Example 2.

**Table 1.** GEM solutions of the distributed instantaneous source strengths of Example 2 with single injection at $t = 0$.

| Time, $t$ (day) | $S_1$ (mg/l) | $S_2$ (mg/l) | $S_3$ (mg/l) |
|---|---|---|---|
| 0 | 80.003 | 550.001 | 179.998 |
| 2 | −.006 | −.003 | .004 |
| 4 | .006 | .000 | −.004 |
| 6 | −.004 | −.004 | .003 |
| 8 | .004 | .005 | −.003 |
| 10 | −.004 | −.004 | .003 |

**Table 2.** True values and GEM solutions of the distributed instantaneous source strengths of Example 2 for various noise levels.

| | | $\varphi = 0\%$ | | $\varphi = 2\%$ | | $\varphi = 5\%$ | |
|---|---|---|---|---|---|---|---|
| Sources | True values (mg/l) | Strength | Relative error (%) | Strength | Relative error (%) | Strength | Relative error (%) |
| $S_1$ (mg/l) | 80.0 | 80.003 | .0 | 79.889 | 1.1 | 79.717 | .35 |
| $S_2$ (mg/l) | 550.0 | 550.001 | .0 | 546.078 | .0 | 540.195 | 1.78 |
| $S_3$ (mg/l) | 180.0 | 179.998 | .0 | 179.493 | .2 | 178.735 | .70 |

is a Neumann one with a normal contaminant flux, $q = .15 \times t$ m.mg/$l$. There is no exact solution for this problem, so a direct GEM simulation of the problem is implemented with pollution source strength $S_1 = 80.0$ mg/$l$, $S_2 = 550.0$ mg/$l$ and $S_3 = 180.0$ mg/$l$. The domain is discretised into 384 uniform rectangular elements each [$\Delta x = 50$ m $\times$ $\Delta y = 50$ m], a uniform time step $\Delta t = 2.0$ days, and a weighting factor, $\theta = 1.0$ are adopted in the simulations. The results from the direct GEM simulation are used as estimates of the concentration values at six

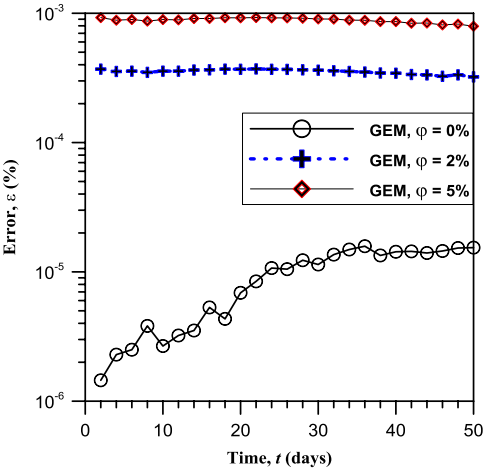


**Figure 9.** Error plots of the GEM predicted contaminant plume with time for single injection from distributed sources.

observation points at (200 m, 600 m), (350 m, 700 m), (750 m, 100 m), (800 m, 250 m), (1000 m, 600 m) and (1000 m, 750 m).

The results of the inverse GEM simulations in predicting the distributed instantaneous sources are presented in Table 1, and they indicate accurate prediction of their strengths with no residual values at subsequent simulation times. Noise levels of 2 and 5% are introduced into the observed data, and the predicted distributed source strengths are compared to the true values in Table 2. It is observed that the maximum relative error in the prediction of the source strength is 1.78% at noise level of 5%, and this shows that introducing noise in the data has little influence on the source strength prediction.

The errors of the inverse GEM solutions for the contaminant plume in relation to those from the direct GEM simulations are calculated by Equation (19) and presented in Figure 9. The errors are very small, indicating that the inverse and direct GEM solutions are quite identical. The contaminant plumes of the GEM solutions are presented in Figure 10 at $t = 6$ days and 36 days. The range of values of the regularisation parameter used in the simulations is from $9.12 \times 10^{-7}$ to $4.47 \times 10^{-5}$ with an average value of $1.72 \times 10^{-5}$.

### *4.2.2. Multiple injection episodes*

This example is similar to that under Section 4.2.1, except that injections of the pollutants into the aquifer at the three distributed locations occur at $t = 0$, $t = 26$ days and $t = 44$ days. The strengths of the pollutants being injected vary over the times of injections. At $t = 0$, the strengths of $S_1$, $S_2$ and $S_3$ are the same as in the previous case, while at $t = 26$ days, $S_1 = 30.0$ mg/$l$, $S_2 = 700.0$ mg/$l$ and $S_3 = 115.0$ mg/$l$ and at $t = 44$ days, $S_1 = 60.0$ mg/$l$, $S_2 = 470.0$ mg/$l$ and $S_3 = 140.0$ mg/$l$. These source strengths are used in the direct GEM formulation to generate the solution for the

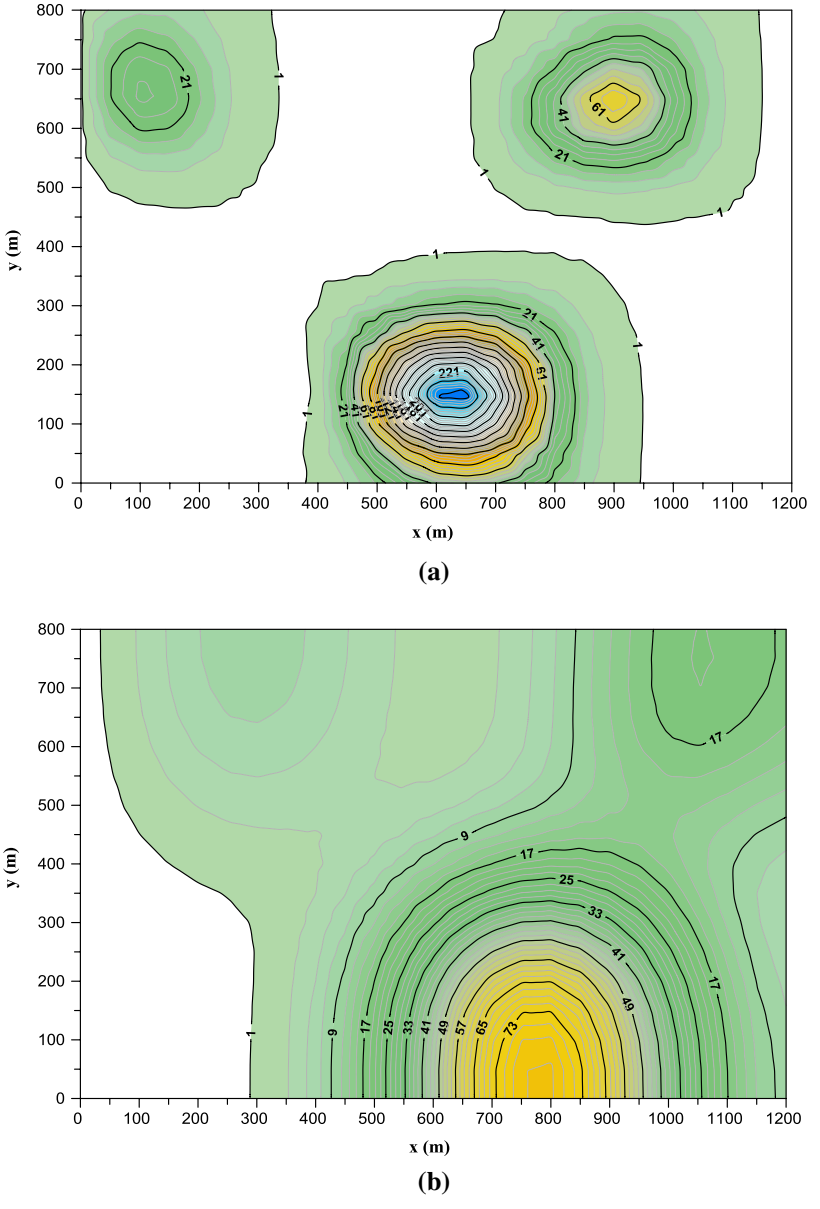


**Figure 10.** Contaminant plumes from the GEM simulations: (a) $t = 6$ days, (b) $t = 36$ days for single injection from distributed sources.

concentration at the six observation points that are at the same locations as in the previous case. The computational domain, medium parameters remain the same, while the inverse formulation presented herein is used to predict the three source strengths. The results of the true values of the distributed source strengths and their simulated values are presented in Table 3 for the second and third episodes of pollutant injections into the aquifer at noise levels of 0, 2 and 5%. It should be noted that the results for the first episode of injection is the same as that in Table

**Table 3.** True values and GEM solutions of the distributed instantaneous source strengths of Example 2 with multiple injection episodes for various noise levels.

| Injection Episodes | Sources | True values (mg/l) | $\varphi = 0\%$ | | $\varphi = 2\%$ | | $\varphi = 5\%$ | |
|---|---|---|---|---|---|---|---|---|
| | | | Strength | Relative error (%) | Strength | Relative error (%) | Strength | Relative error (%) |
| Second injection at $t$ = 26 days | $S_1$ | 30 | 30.004 | .01 | 29.963 | .12 | 29.898 | .34 |
| | $S_2$ | 700 | 700.02 | .00 | 694.983 | .72 | 687.471 | 1.79 |
| | $S_3$ | 115 | 114.997 | .00 | 114.705 | .26 | 114.268 | .64 |
| Third injection at $t$ = 44 days | $S_1$ | 60 | 59.999 | .00 | 59.917 | .14 | 59.791 | .35 |
| | $S_2$ | 470 | 469.945 | .01 | 466.661 | .71 | 461.775 | 1.75 |
| | $S_3$ | 140 | 140 | .00 | 139.576 | .30 | 138.947 | .75 |

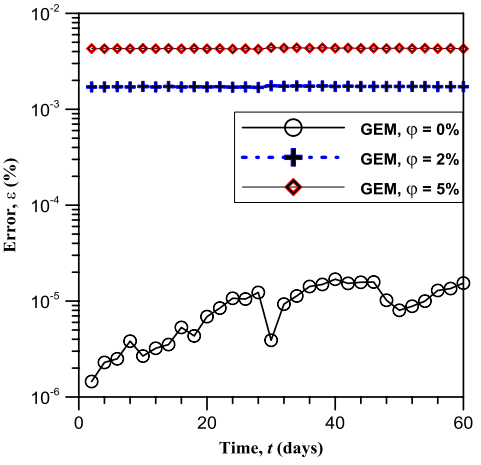


**Figure 11.** Error plots of the GEM predicted contaminant plume with time for multiple injection episodes from distributed sources.

2. With no noise in the observation data, the inverse GEM reproduced the true values of the source strengths, while the maximum relative error of 1.79% in the prediction of the source strength is observed for 5% noise level. The results do indicate that the GEM formulation is accurate and robust in predicting the source strengths of distributed sources with multiple pollutant injections.

The error variation with time for the inverse GEM solutions in comparison with the direct GEM solutions are presented in Figure 11, and it shows that that the errors are small for the noise levels of 0, 2 and 5%, indicating that the inverse and direct GEM solutions are essentially identical. The contaminant plume of the GEM solutions, presented in Figure 12 at $t$ = 36 days, is significantly different from the plume in Figure 10(b) when there is a single episode of pollution injection into the aquifer. The values of the regularisation parameter that are used in the simulations range between $9.21 \times 10^{-7}$ and $2.90 \times 10^{-5}$ with an average value of $1.32 \times 10^{-5}$.

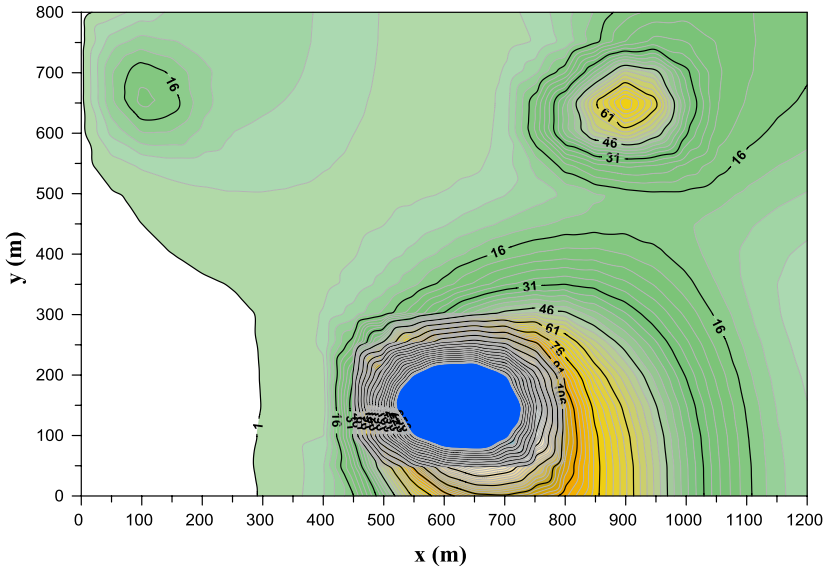


**Figure 12.** Contaminant plume from the GEM simulations at $t = 36$ days for multiple injection episodes from distributed sources.

## 5. Conclusion

The inverse Green element solutions of the advection-dispersion equation have been presented for the problem of predicting the source strengths when pollution is instantaneously injected from point and distributed sources into an aquifer. The numerical solutions were obtained for both a single episode of injection and multiple episodes of pollution injections into the aquifer. The over-determined, ill-conditioned global matrix generated in the numerical formulation is solved by the least squares method and regularised by the Tikhonov technique. Two numerical examples are used to demonstrate the computational capabilities of the GEM formulation. The first example, which has an analytical solution, dealt with the estimation of the strengths of four instantaneous point pollution sources, while the second addressed the problem of estimation of three distributed pollution sources. The current formulation is capable of estimating the multiple instantaneous source strengths from concentration data of contaminant plumes. The capability of the method to estimate the source strengths when there are multiple episodes of pollution injections demonstrates its robustness. It is observed that GEM gives better prediction of distributed pollution sources than point sources, and this is due to the spatial and temporal discontinuities associated with the latter. Errors associated with measurement data at observation points do not have much influence on the prediction of the distributed instantaneous pollution source strengths. Although both examples addressed in this paper used uniform velocity flow fields in the numerical simulations, future work is being carried out to implement the current GEM formulation for non-uniform flow cases.

## Disclosure statement

No potential conflict of interest was reported by the author.

## References

Atmadja, J., & Bagtzoglou, A. C. (2001). Pollution source identification in heterogeneous porous media. *Water Resources Research, 37*, 2113–2125.

Bear, J. (1979). *Hydraulics of groundwater*. New York, NY: McGraw Hill.

Brebbia, C. A. (1978). *The boundary element method for engineers*. Great Britain: Pentech Press.

Cokca, E., Bilge, H. T., & Unutmaz, B. (2009). Simulation of contaminant migration through a soil layer due to an instantaneous source. *Computer Applications in Engineering Education, 19*, 385–398.

Datta, B., Chakrabarty, D., & Dhar, A. (2011). Identification of unknown groundwater pollution sources using classical optimization with linked simulation. *Journal of Hydro-environment Research, 5*, 25–36.

Hansen, P. C. (1994). Regularization tools: A Matlab package for analysis and solution of discrete ill-posed problems. *Numerical Algorithms, 6*, 1–35.

Jha, M., & Datta, B. (2013). Three-dimensional groundwater contamination source identification using adaptive simulated annealing. *Journal of Hydrologic Engineering, 18*, 307–317.

Michalak, A. M., & Kitanidis, P. K. (2004). Estimation of historical groundwater contaminant distribution using the adjoint state method applied to geostatistical inverse modeling. *Water Resources Research, 40*, W08302. doi:10.1029/2004WR003214

Neupauer, R. M., & Lin, R. (2006). Identifying sources of a conservative groundwater contaminant using backward probabilities conditioned on measured concentrations. *Water Resources Research, 42*, W03424. doi:10.1029/2005WR004115

Onyari, E., & Taigbenu, A. (2017). Inverse Green element evaluation of source strength and concentration in groundwater contaminant transport. *Journal of Hydroinformatics, 19*, 81–96. doi:10.2166/hydro.2016.028

Sun, A. Y., Painter, S. L., & Wittmeyer, G. W. (2006a). A constrained robust least squares approach for contaminant source release history identification. *Water Resources Research, 42*, W04414. doi:10.1029/2005WR004312

Sun, A. Y., Painter, S. L., & Wittmeyer, G. W. (2006b). A robust approach for contaminant source location and release history recovery. *Journal of Contaminant Hydrology, 88*, 29–44.

Taigbenu, A. E. (2012). Enhancement of the accuracy of the Green element method: Application to potential problems. *Engineering Analysis with Boundary Elements, 36*, 125–136.